Revista GEOCIÊNCIAS

unesp

ISSN: 1980-900X (online)

ITAPECERICA METAMAFIC-ULTRAMAFIC ROCKS WITH E-MORB SIGNATURE: OPHIOLITIC REMNANTS OF THE RHYACIAN-OROSIRIAN OROGENY IN SOUTHERN SÃO FRANCISCO CRATON?

ROCHAS METAMÁFICAS-ULTRAMÁFICAS COM ASSINATURA E-MORB NA REGIÃO DE ITAPECERICA: REMANESCENTES OFIOLÍTICOS DA OROGENIA RHYACIANA-OROSIRIANA NO SUL DO CRÁTON SÃO FRANCISCO?

Daniel Andrade MIRANDA, Alexandre de Oliveira CHAVES

Universidade Federal de Minas Gerais. Instituto de Geociências. Avenida Presidente Antônio Carlos, 6627 - Pampulha, Belo Horizonte – MG. E-mail: miranda.geologia@gmail.com; alochaves@yahoo.com.br

ABSTRACT - In the Southern São Francisco Craton near Itapecerica (Minas Gerais – Brazil) occurs a supracrustal succession of rocks, varying from bottom to top by quartzite, graphite schist, khondalitic paragneiss and banded iron formation whose protoliths are from oceanic basin with ages in the context of the Rhyacian-Orosirian orogeny. Amphibolite and metaultramafic bodies occur associated to this succession. Mineralogical and textural features of the amphibolite allow suggesting a gabbroic protolith metamorphosed to granulite facies and retrometamorphosed in amphibolite facies to generate the amphibolite. Geochemistry reveals tholeiitic affinity to the amphibolite protolith, which has an E-MORB signature, associating this rock to an oceanic setting. The association of amphibolite to metaperidotite in oceanic setting suggest the transition of gabbro to ultramafic rocks in a typical ophiolite sequence. A possible suture zone in the Itapecerica/Claudio region formed by the collision between Divinopolis and Campo Belo/Bonfim complexes during the Rhyacian-Orosirian orogeny involving the Itapecerica oceanic basin alongside Claudio Shear Zone and forward to Minas Basin is a suggestive geological setting of the investigated region.
Keywords: Amphibolite. Metaperidotite. Ophiolite. Petrology. São Francisco Craton.

RESUMO - No sul do Cráton São Francisco, próximo a Itapecerica (Minas Gerais - Brasil), ocorre uma sucessão de rochas supracrustais, variando da base para o topo por quartzito, grafita xisto, paragnaisse kondalítico e formação ferrífera bandada cujos protólitos são de bacia oceânica com idades no contexto da orogenia Riaciano-Orosiriana. Corpos anfibolíticos e metaultramáficos ocorrem associados a esta sucessão. As características mineralógicas e texturais do anfibolito permitem sugerir um protólito gabroico metamorfizado em fácies granulito e retrometamorfizado em fácies anfibolito para gerar o anfibolito. A geoquímica revela afinidade toleítica para o protólito do anfibolito, que possui uma assinatura E-MORB, associando esta rocha a um ambiente oceânico. A associação de anfibolito a metaperidotito em ambiente oceânico sugere a transição de gabro para rocha ultramáfica em uma sequência típica de ofiolito. Uma possível zona de sutura na região de Itapecerica/Claudio formada pela colisão entre os complexos Divinópolis e Campo Belo/Bonfim durante a orogenia Riaciano-Orosiriana, envolvendo a bacia oceânica de Itapecerica ao lado da Zona de Cisalhamento Claudio e em direção a Bacia Minas é um ambiente geológico sugestivo para a região investigada.
Palavras-chave: Anfibolito. Metaperidotito. Ofiolito. Petrologia. Cráton São Francisco.

INTRODUCTION

Ophiolites are fragments of oceanic lithosphere with fundamental constraints on the reconstruction of the evolution of an ancient oceanic basin and surrounding continental areas (Saccani, 2015). They form in a wide variety of tectonic settings including oceanic spreading ridges, hot spots, and suprasubduction zone (SSZ) environments such as intra-oceanic arcs, continental arcs, forearcs and back-arcs (Dilek & Furnes, 2011).

In the Southern São Francisco Craton near Itapecerica (Minas Gerais, Brazil) occurs a supracrustal succession of rocks, varying from bottom to top, constituted by quartzite (partly ferruginous with laminar graphite), graphite schist interlayered with quartzite bands and khondalitic paragneiss (Carneiro et al., 2007; Campello et al., 2015). Recent radiometric dating of these rocks linked them to the Rhyacian-Orosirian orogeny (monazite U-Th-Pb_T mean age of 2010 ± 19 Ma (Chaves et al., 2015); a maximum deposition age of 2080 Ma and a metamorphic overprint on granulite facies of 2069 ± 84 Ma (Teixeira et al., 2017a); monazite

U-Th-Pb$_T$ age of 2090 ± 26 Ma corresponding to metamorphic peak and 1937 ± 32 Ma to orogen collapse (Miranda et al., 2020)). Amphibolite and metaultramafic bodies occur in this succession.

The tectonic model proposed by Miranda et al. (2019) includes the Itapecerica supracrustal succession in the Rhyacian-Orosirian orogeny alongside Paleoproterozoic Minas Supergroup involved in a progressive compressional deformation, which resulted in a fold-thrust belt developed by the collision of the São Francisco paleoplate nucleus with other terranes, and ultimately with the Congo paleoplate nucleus at ca. 2100 Ma or immediately after (Dutra et al., 2019).

The possibility that these metamafic-ultramafic rocks represent remnants of an ophiolite could constrain the tectonic setting of the Itapecerica region.

This paper consists of a petrologic study of these rocks using petrography and whole-rock chemical composition to classify and identify the geochemical affinity and the tectonic environment of the amphibolites and metaultramafic rocks from Itapecerica supracrustal succession.

GEOLOGICAL SETTING

The southern part of São Francisco Craton (SFC) (Figure 1A) consists of Archean crust (3.2–2.6 Ga) composed mainly of granite-gneisses (Farina et al., 2015; Teixeira et al., 2017b), greenstone belts (Rio das Velhas Supergroup), Paleoproterozoic clastic-chemical metasedimentary rocks (including the banded iron formations of the Quadrilátero Ferrífero (QF) mining district from Minas Supergroup), and Neoproterozoic pelitic-carbonate sedimentary rocks from Bambuí Group (Teixeira et al., 2017b).

The Archean granite-gneiss basement of the southern SFC is subdivided in distinct metamorphic complexes, named as Divinópolis, Campo Belo/Bonfim and Belo Horizonte (Machado Filho et al., 1983; Teixeira et al., 1996). (Figure 1B).

The Minas Supergroup extends to the SW of the QF, as portrayed by the correlative strata along the Jeceaba-Bom Sucesso lineament (Neri et al., 2013). Mafic dykes of several generations crosscut the southern SFC (Chaves, 2013).

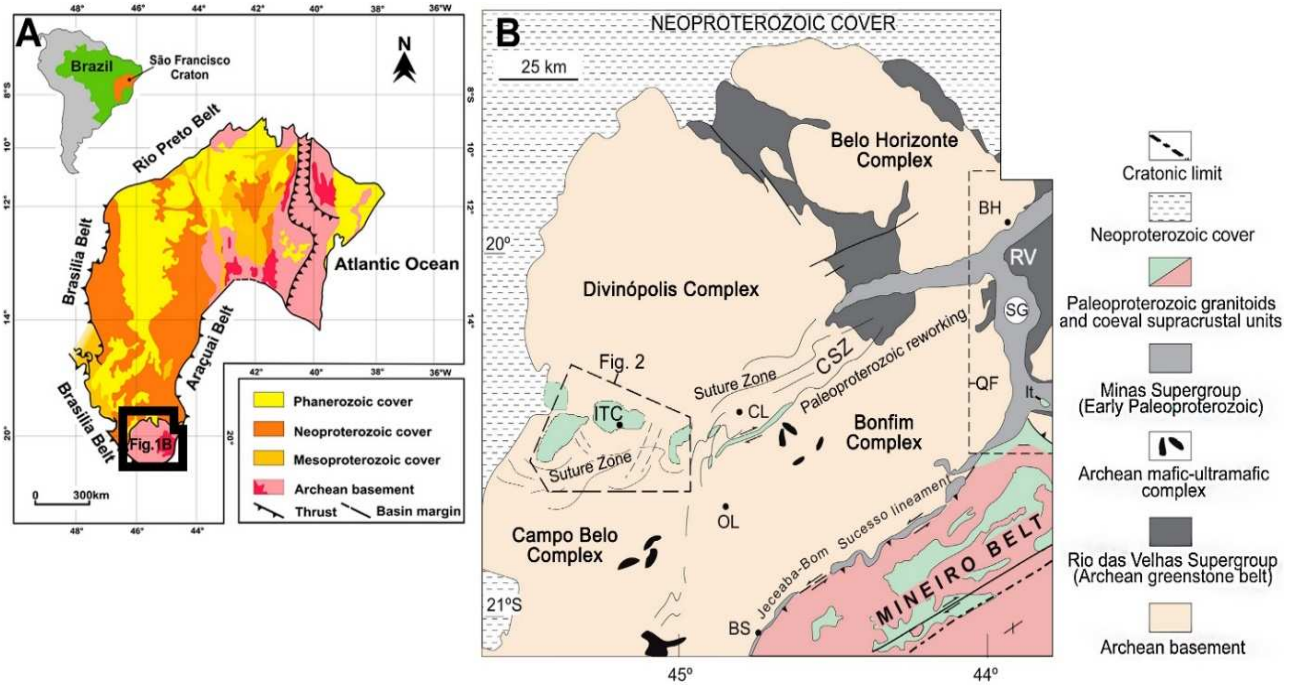

Figure 1 - (A) Sao Francisco Craton location. Modified from Drummond et al. (2015). (B) Geological map of the southern portion of the Sao Francisco Craton. Keys: RV = Neoarchean Rio das Velhas Supergroup; SG = Sabará Group (Early Paleoproterozoic Minas Supergroup); It = Itacolomi Group (<1.96 Ga); CSZ = Cláudio Shear Zone; QF = Quadrilátero Ferrifero mining district. Towns: ITC (Itapecerica), CL (Cláudio), OL (Oliveira), BS (Bom Sucesso), BH (Belo Horizonte). Modified from Teixeira et al. (2017a).

The Rhyacian-Orosirian orogeny amalgamated Archean nucleus and different continental to oceanic arcs that collided to form the proto-SFC (Aguilar et al., 2017; Moreira et al., 2018). It is related to the deformation of the Minas Supergroup, to the accretion of juvenile crust that formed the Mineiro Belt to the southeast (Noce et al., 1998; Ávila et al., 2014; Teixeira et al.,

2015) and was responsible for extensive reworking of terranes located at the margins of the craton (Noce et al., 2007). In the interior of the southern SFC Archean core, occur the Água Rasa metagranite (1934 ± 74 Ma from zircon U-Pb) and khondalites (monazite U-Th-Pb_T dating of 2090 ± 26 Ma and 1937 ± 32 Ma) from the Itapecerica supracrustal succession (Miranda et al., 2020). In addition, near the Cláudio Shear Zone (CSZ), amphibolites with E-MORB signature have igneous protolith crystallization U-Pb age of 2159 ± 21 Ma and metamorphic recrystallization age between 2.06 Ga and 2.03 Ga (Goulart, 2006; Goulart & Carneiro, 2010), confirming the existence of a Paleopro-terozoic event in the region between the Archean Divinópolis and Campo Belo/Bonfim granite-gneiss metamorphic complexes (Figure 1B).

The study area is located in the crystalline basement of the Itapecerica region (Figure 1B). According to Carneiro & Barbosa (2008), the area contains gneisses, metagranitoids, amphibolites, mafic, metaultramafic and metacharnockitic rocks formed in the Mesoarchean and recrystallized under high amphibolite- to granulite facies conditions (Fernandes & Carneiro, 2000). The elliptical geophysical anomalies (Figure 2A, 2B) hosting the second largest graphite mine in Brazil are located to the west of the CSZ around Itapecerica town.

The Água Rasa Metagranite (Miranda et al., 2020) constitutes the perimeter of the elliptical anomalies.

The country rocks that surround the Água Rasa Metagranite and the Itapecerica metasedimentary rocks (Figure 2A) are distinguished as the Neoarchean Candeias (Campo Belo Complex) and Paleoproterozoic Itapecerica gneissic units (Divinopolis Complex). Both units show variable migmatization (Oliveira, 2004; Campello et al., 2015).

The Divinópolis complex is composed predominantly of greyish TTG (tonalitic-trondhjemitic-granodioritic) orthogneisses with variable migmatization and Campo Belo/Bonfim complex has tonalitic-granodioritic composition with instrusions of 2790–2610 Ma granitoids and minor occurrence of metaultramafic-mafic rocks (Fernandes & Carneiro, 2000; Oliveira, 2004; Romano et al., 2013; Campello et al., 2015; Farina et al., 2015). The Archean Candeias Gneiss is part of the Campo Belo complex and is essentially greenish granulitic gneisses with granodioritic (charnoenderbites) to granitic (charnockites) composition and variable migmatization (Oliveira, 2004; Carneiro et al., 2007).

The Paleoproterozoic Itapecerica migmatitic gneiss is here interpreted as formed by crustal reworking of the Divinópolis complex and Paleoproterozoic supracrustal sequences during Rhyacian-Orosirian Orogeny.

According to Carneiro et al. (2007), it is a locally migmatized pinkish gneiss with peraluminous affinity and shows granitic to granodioritic composition. The 2.04 Ga Kinawa migmatite of the Itapecerica Metamorphic Complex (Carvalho et al., 2017) is an example of reworked crust, in which ~2.7 Ga metagranodiorites of the Campo Belo/Bonfim Metamorphic Complex were partially melted in the Cláudio Shear Zone (CSZ) during the Paleoproterozoic.

The Itapecerica graphite-rich metasediment-tary rocks, amphibolite and meta-ultramafic bodies occur together inside the elliptical geophysical anomalies (Figure 2B; Figure 3A, 3B). The Itapecerica metasedimentary rocks essentially consist of khondalite paragneiss and minor lenticular graphite schist that is interlayered with quartzite bands (partly ferruginous with laminar graphite) and locally marble rocks (Figure 3C). In particular, the khondalite exhibits compositional layering and local anatexis and may contain thin graphite films (Carneiro et al., 2007; Campello et al., 2015).

The Itapecerica metasedimentary rocks went through of amphibolite to granulite facies metamorphic conditions during continental collision with crustal thickening followed by tectonic exhumation and a post-peak decompressional stage due to orogen collapse (Miranda et al., 2020), and are strongly deformed (Teixeira et al., 2017a). In the surroundings are reported the occurrence of banded iron formation (Figure 3D). Teixeira et al. (2017a) conducted isotopic studies on the Itapecerica graphite-rich supracrustal succession and the detrital zircon analyses in paragneiss indicated a maximum deposition age of 2080 Ma and a metamorphic overprint on granulite facies of 2069 ± 84 Ma (Figure 2). Chaves et al. (2015) previously reported monazite electron microprobe chemical data in the paragneisses that yielded a U-Th-Pb_T mean age of 2010 ± 19 Ma.

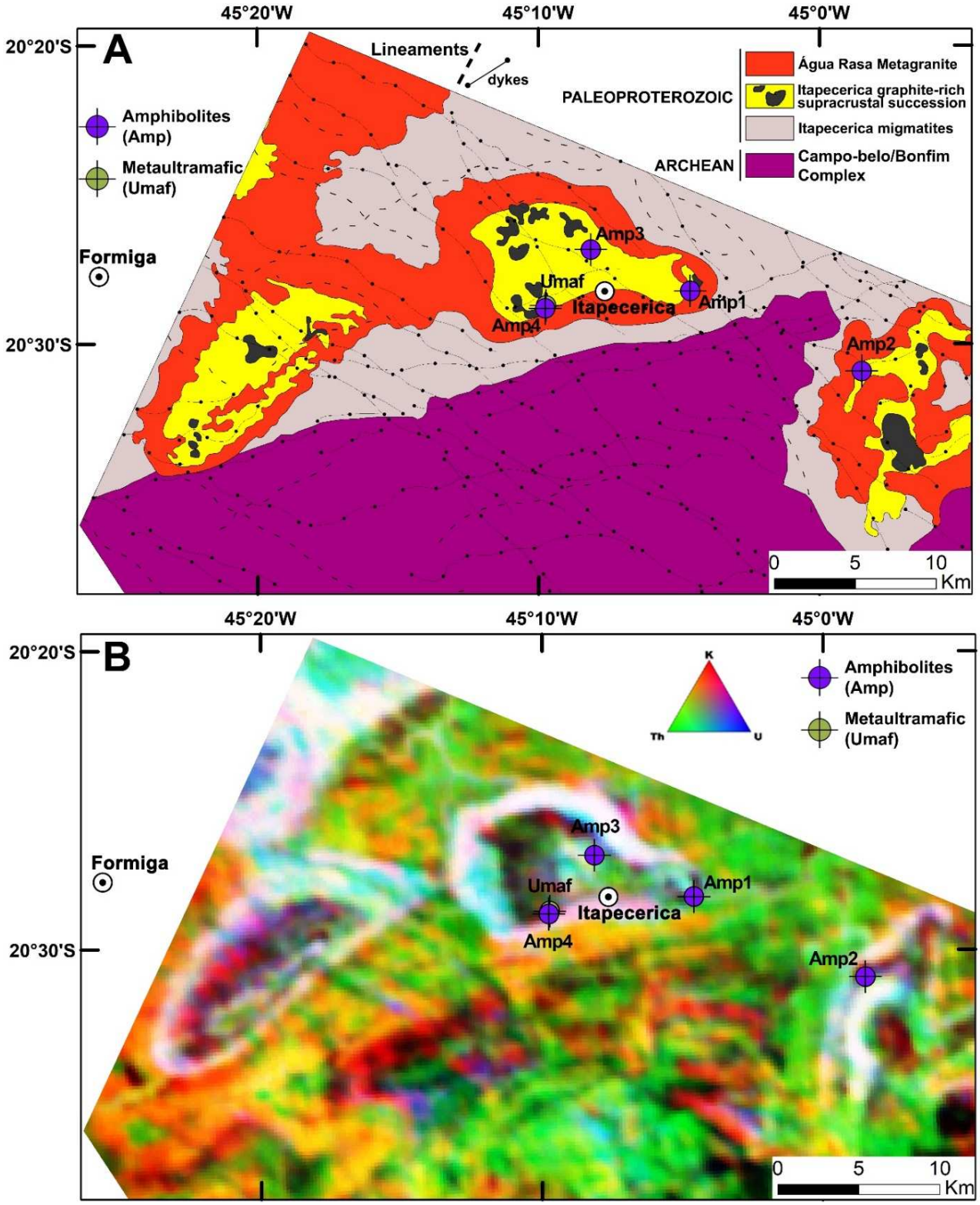

Figure 2 - (A) Simplified geological map with samples sites. Amphibolite bodies are shown in black inside Itapecerica graphite-rich supracrustal succession. (B) Gammaespectrometry U-Th-K map. Addapted from Ruy et al. (2006) and Zacchi et al. (2007).

METHODS

Four petrographic thin sections from four samples of amphibolites and one of the metautramafic rock were made in the laboratories of the Geosciences Institute at Federal University of Minas Gerais (IGC/UFMG), and the same five samples were sent to the SGS-Geosol Laboratory, where, after tungsten milling, the material was melted with lithium metaborate and dilute nitric digestion. The major elements and five trace elements (Ba, Nb, Sr, Y, Zr) were analyzed by ICP-OES (Optical Emission Spectrometry with Inductively Coupled Plasma).

Other traces, together with fourteen REE,

were analyzed by ICP-MS (Inductively Coupled Plasma Mass Spectrometry). Detection limits were generally around 0.01% for the major elements oxides and 1 ppm for trace and REE. The accuracy is in the range of 1-2% from the relative standard deviation. The loss on ignition (LOI) was determined by the mass difference after heating at 1000 °C. Then, to geochemical data treatment, the Geoplot program (Zhou & Li, 2006) a supplement for Microsoft Excel, was used.

Mineral abbreviations are after Whitney & Evans (2010), including Cpx – clinopyroxene, Hbl – hornblende, Ol – olivine, Opx – orthopyroxene, Pl – plagioclase, Srp – serpentine, Spl – spinel, and Qz – quartz.

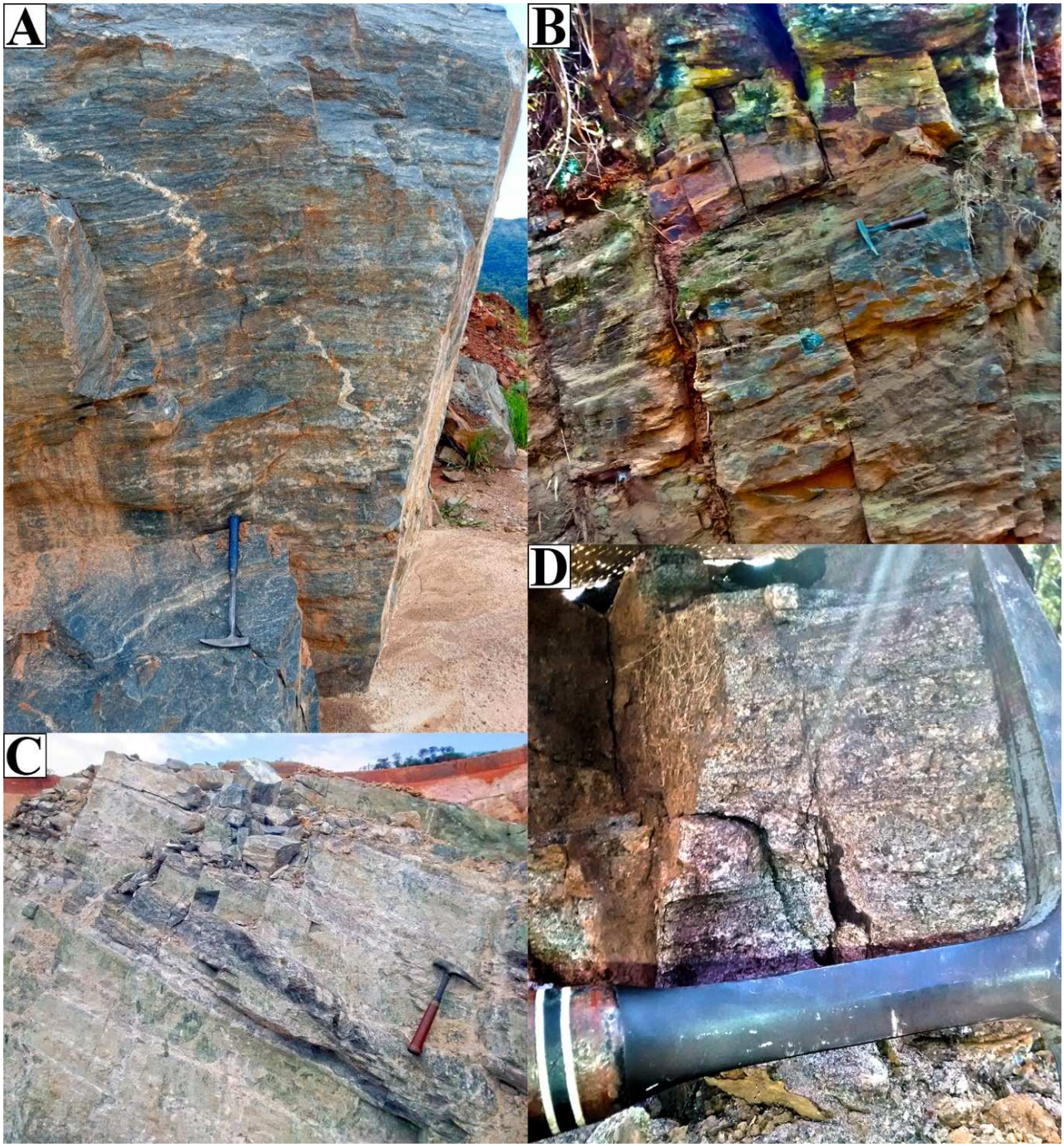

Figure 3 - Sampling sites for amphibolite (A) and metaultramafic (B). (C) Occurrence of marble rocks inside a graphite mine. (D) Banded iron formation nearby Itapecerica.

RESULTS AND DISCUSSIONS

Metaultramafic

During fieldwork, only one outcrop of layered metaultramafic rock was found (Figure 3B) close to amphibolites and rocks of the Itapecerica supracrustal sequence (Figure 2). In thin section, metaultramafic rock also shows layered structure and cumulate texture composed of serpentine (after olivine) cumulus and clinopyroxene and

orthopyroxene intercumulus (Figures 4A, 4B – white dashed lines). The mineral assemblage is composed of serpentine (after olivine) (~50%), clinopyroxene (~25%), orthopyroxene (~20%), and spinel and opaque minerals are the accessory minerals present in this rock. Olivine is serpentinized but some relict crystals are present (Figure 4D). Clinopyroxene appears as fine to medium-sized granoblastic aggregates in subhedral shapes. Orthopyroxene appears as coarse to medium-sized grains in subhedral to anhedral shapes.

The mineralogy allows classifying the rock protolith as a spinel lherzolite according to Streckeisen (1974). The growth of orthopyroxene to coarse grains would have occurred during the amphibolite to granulite facies metamorphism. During the post-peak decompressional stage due to orogen collapse most of the olivine was serpentinized.

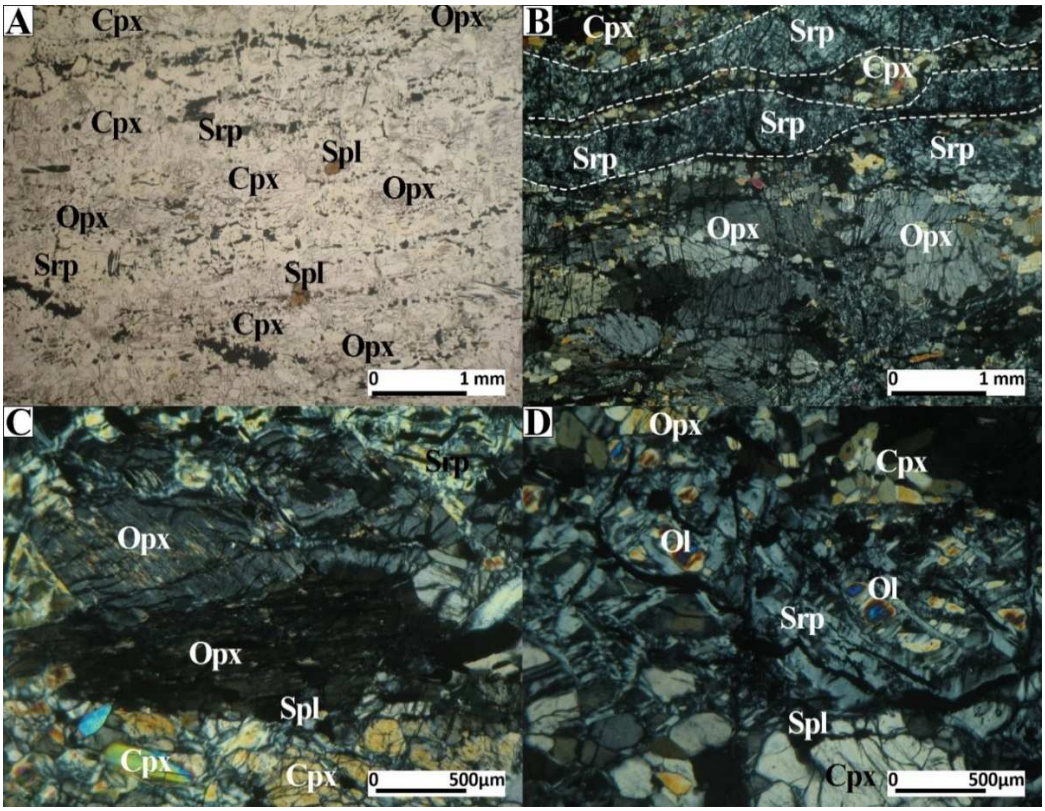

Figure 4 - Photomicrographs (plane-polarized light, PPL; cross-polarized light, CPL) of representative mineral assemblages of the metaultramafic rock. (A) Photomicrograph (PPL) and (B) Photomicrograph (CPL) of the layered structure and cumulate texture. (C) Photomicrograph (CPL) of the two pyroxenes. (D) Photomicrograph (CPL) showing serpentine bands with relict olivine crystals.

Amphibolite

Amphibolite outcrops occur dispersed in the area in association to rocks of the Itapecerica supracrustal sequence (Figure 2). The rock shows continuous centimeter-sized banding (Figure 3A). The amphibolites are usually fine- to medium-grained rocks of granonematoblastic texture. The mineral assemblage is constituted by plagioclase (~40%), hornblende (~40%), clinopyroxene (~20%), and quartz, orthopyroxene and opaques minerals appear as accessories (Figure 5). Plagioclase comprises the felsic portions of granoblastic aggregates. Hornblende defines the foliation, has medium-sized grains with polygonal boundaries and substitutes clinopyroxene (Figure 5), which appears as relict crystal. Orthopyroxene and some quartz occur replacing clinopyroxene.

Mineralogical and textural features points out to a gabbroic protolith that was metamorphosed in granulite facies conditions, followed by retrometamorphism recorded by the clinopyroxene being replaced by hornblende (Figure 5).

Whole-Rock geochemistry

The results of whole-rock geochemistry for the amphibolite and metaultramafic samples are listed on the Table 1. In terms of major components for the amphibolites, the SiO_2 concentration range from 50.06 to 51.94 (wt. %), $Na_2O + K_2O$ from 2.34 to 3.07 (wt. %) and Mg# ratios are between 45.8-59.7, and the metaultramafic has Mg# ratio of 88.4.

The amphibolite samples are classified as subalkaline tholeiitic basalt using the SiO_2 vs Nb/Y

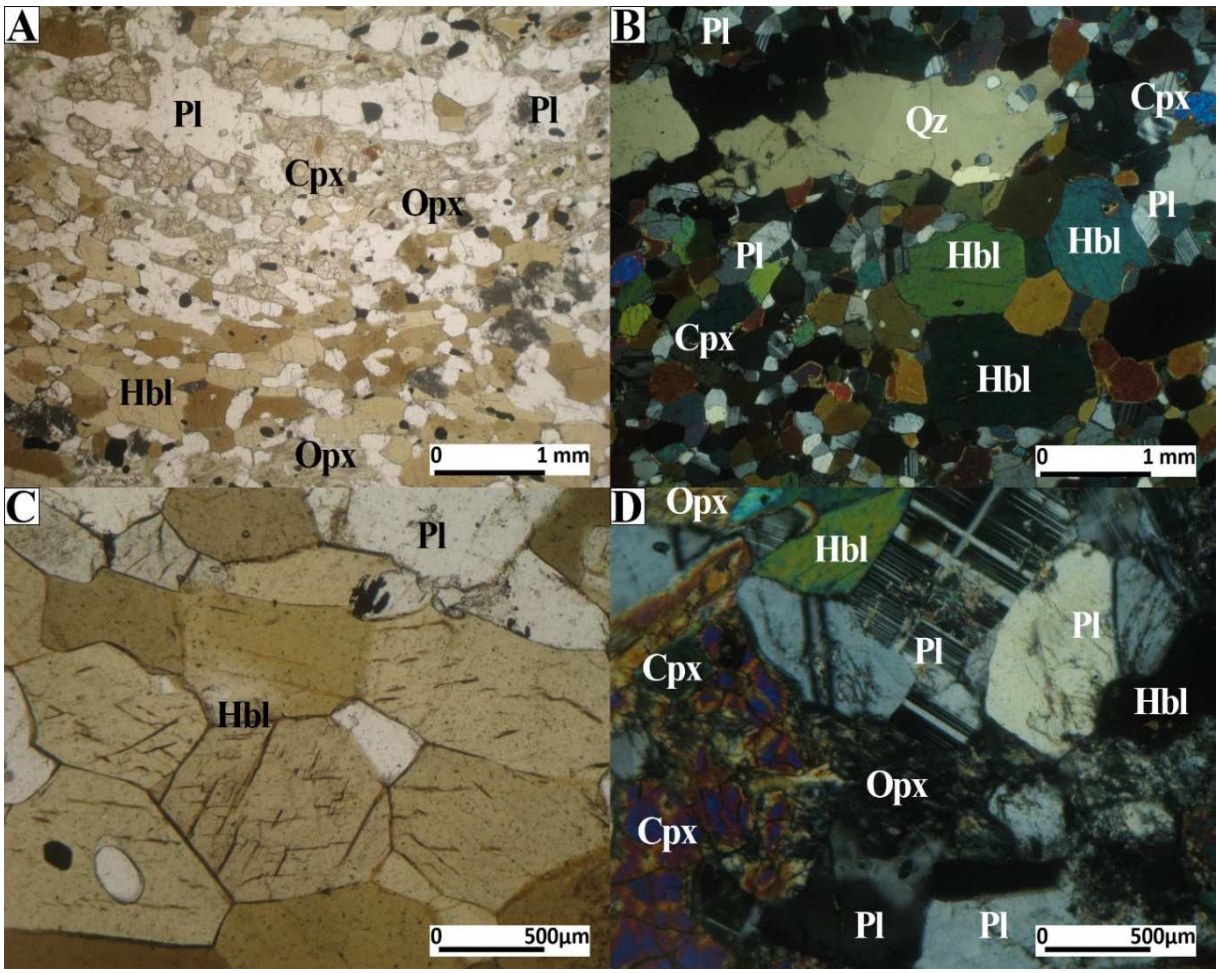

Figure 5 - Photomicrographs (plane-polarized light, PPL- A, C, D; cross-polarized light, CPL - B) of representative mineral assemblage of the amphibolite.

Table 1 – Bulk rock compositions for the amphibolite and metaultramafic samples.

Sample	Major Elements (%)												
	SiO_2	TiO_2	Al_2O_3	FeO_T	MnO	MgO	CaO	Na_2O	K_2O	P_2O_5	Cr_2O_3	Lol	Total
	detection limit 0.01 %												
Amp1	51.63	1.89	14.20	12.13	0.30	4.39	11.86	2.84	0.23	0.19	0.03	0.16	99.85
Amp2	51.94	0.80	14.30	10.12	0.17	6.43	11.54	2.32	0.24	0.07	0.07	0.45	98.45
Amp3	51.18	1.09	13.98	10.14	0.20	6.20	11.16	2.21	0.27	0.12	0.04	0.45	97.04
Amp4	50.60	1.98	13.53	15.43	0.33	6.14	8.22	1.95	0.39	0.18	0.01	0.41	99.17
Umaf	45.78	0.20	4.50	9.19	0.14	30.00	3.02	0.08	0.04	0.01	0.36	7.07	100.39
TILL-3 standard	71.94	0.52	12.21	3.76	0.07	1.66	2.57	2.86	2.35	0.12	0.02	-	98.08

	Trace Elements (ppm)														
	Rb	**Ba**	**Sr**	**Zr**	**Nb**	**Y**	**Ni**	**Co**	**Hf**	**Ta**	**Th**	**U**	**V**	**Cu**	**Ga**
detection limit (ppm)	**0.20**	**10.00**	**10.00**	**10.00**	**0.05**	**0.05**	**5.00**	**0.50**	**0.05**	**0.05**	**0.10**	**0.05**	**5.00**	**5.00**	**0.10**
Amp1	3.30	72.00	228.00	143.00	5.92	38.84	106.00	42.40	3.65	0.29	0.80	0.24	325.00	55.00	14.00
Amp2	4.20	36.00	171.00	62.00	1.64	15.75	109.00	38.40	1.51	0.05	0.30	0.13	214.00	96.00	9.90
Amp3	6.40	58.00	129.00	117.00	3.20	25.09	77.00	38.50	2.47	0.09	0.60	0.26	243.00	115.00	11.20
Amp4	5.70	27.00	136.00	131.00	3.64	35.77	71.00	47.50	3.06	0.10	0.60	0.20	389.00	41.00	14.20
Umaf	1.60	10.00	48.00	25.00	0.53	5.03	1767.00	96.40	0.45	0.05	0.40	0.05	50.00	5.00	4.10
TILL-3 standard	53.20	459.00	310.00	240.00	6.54	-	47.00	14.30	-	0.42	4.20	1.94	70.00	27.00	13.70

	Rare Earth Elements (ppm)													
	La	**Ce**	**Pr**	**Nd**	**Sm**	**Eu**	**Gd**	**Tb**	**Dy**	**Ho**	**Er**	**Tm**	**Yb**	**Lu**
detection limit (ppm)	**0.10**	**0.10**	**0.05**	**0.10**	**0.10**	**0.05**	**0.05**	**0.05**	**0.05**	**0.05**	**0.05**	**0.05**	**0.10**	**0.05**
Amp1	12.90	19.20	3.23	16.50	5.00	1.76	6.84	1.13	7.35	1.61	4.59	0.66	4.30	0.65
Amp2	5.80	10.90	1.47	6.80	1.90	0.74	2.53	0.41	2.82	0.63	1.76	0.26	1.80	0.25
Amp3	10.80	16.90	2.31	10.90	3.00	1.03	4.00	0.68	4.53	0.96	2.88	0.41	2.70	0.40
Amp4	9.80	16.60	2.44	12.90	4.00	1.40	5.76	0.99	6.47	1.40	4.07	0.58	4.00	0.58
Umaf	3.10	3.10	0.60	2.40	0.50	0.23	0.87	0.14	0.89	0.17	0.52	0.07	0.50	0.07
TILL-3 standard	19.60	40.50	4.49	17.60	3.20	0.90	2.95	0.44	2.61	0.48	1.46	0.21	1.40	0.21

diagram (Xia & Li, 2019) and AFM diagram (Irvine & Baragar, 1971 - Figure 6A, 6B). In Jensen diagram (Jensen, 1976 - Figure 6C), amphibolite samples are classified as high-Fe tholeiites and the metaultramafic has komatiitic composition. In V vs Ti/100 diagram (Shervais, 1982), log(Sr/V) *vs* log((Na$_2$O*100)/Ga) diagram (Zhang et al., 2019) and log(Nb/Y) vs log((K$_2$O*100)/Cu) diagram (Zhang et al., 2019) shown in figure 7, amphibolites are classified as mid-ocean ridge basalts (MORB).

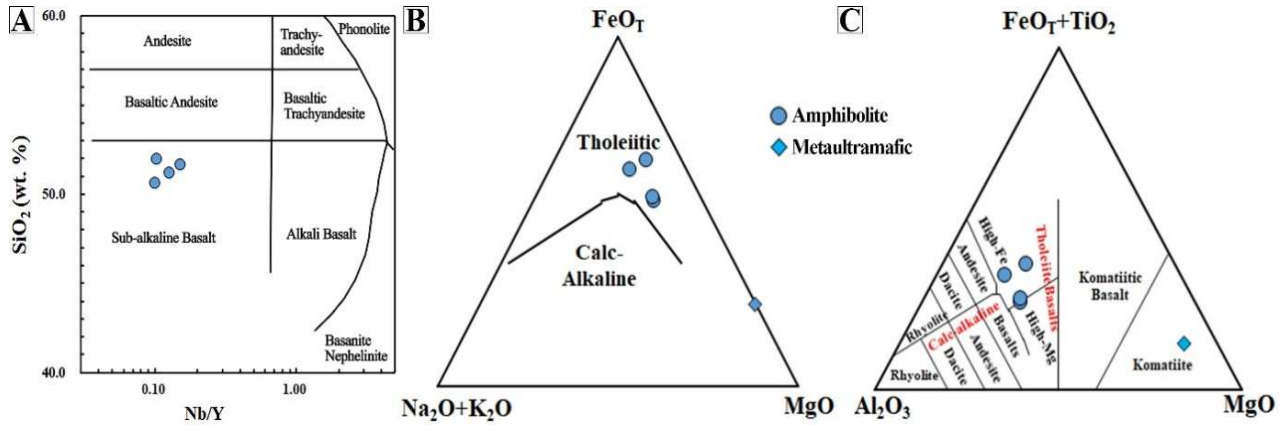

Figure 6 - (A) SiO_2 vs Nb/Y diagram (Xia & Li, 2019). (B) AFM diagram (Irvine & Baragar, 1971). (C) diagram from Jensen (1976).

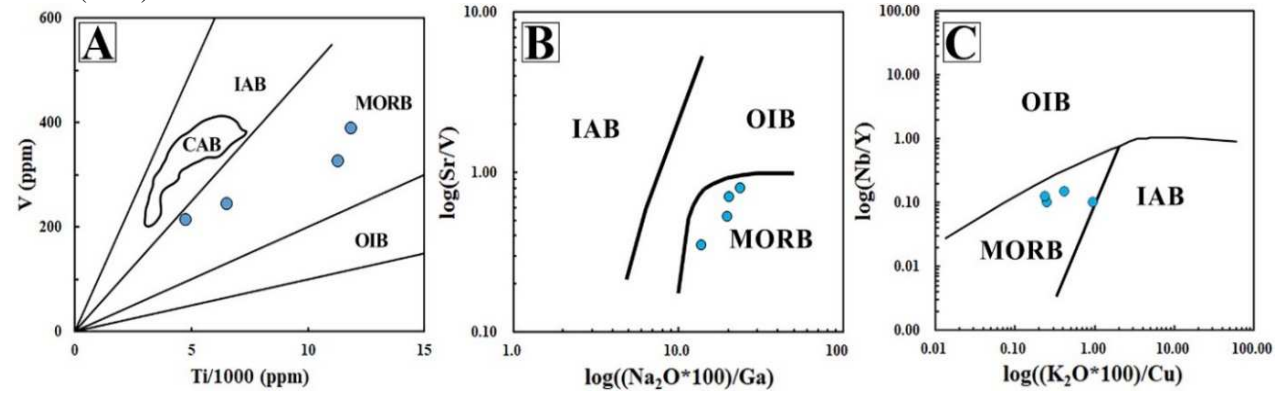

Figure 7 - (A) V vs Ti diagram (Shervais, 1982). (B) log(Sr/V) vs log((Na$_2$O*100)/Ga) diagram (Zhang et al., 2019). (C) log(Nb/Y) vs log((K$_2$O*100)/Cu) diagram (Zhang et al., 2019). CAB – Calc-alkaline basalts, IAB – Island arc basalts, OIB – Ocean island basalts, MORB – Mid-ocean ridge basalts. Only amphibolite samples were ploted.

Amphibolites show similar to enriched-MORB (E-MORB) pattern in both chondrite-normalized REE and primitive mantle-normalized multi-element diagrams, but with negative anomalies in Nb and Ta (Figure 8A, 8B). They have $(La/Yb)_N$ between 1.76-2.87 and a poorly fractionated light rare earth elements (LREE) distribution pattern [$(La/Sm)_N$ = 1.58-2.32] and flat heavy rare earth elements (HREE) distribution [$(Gd/Yb)_N$ = 1.16-1.32]. The patterns of the amphibolite are very similar to that of metaultramafic rock.

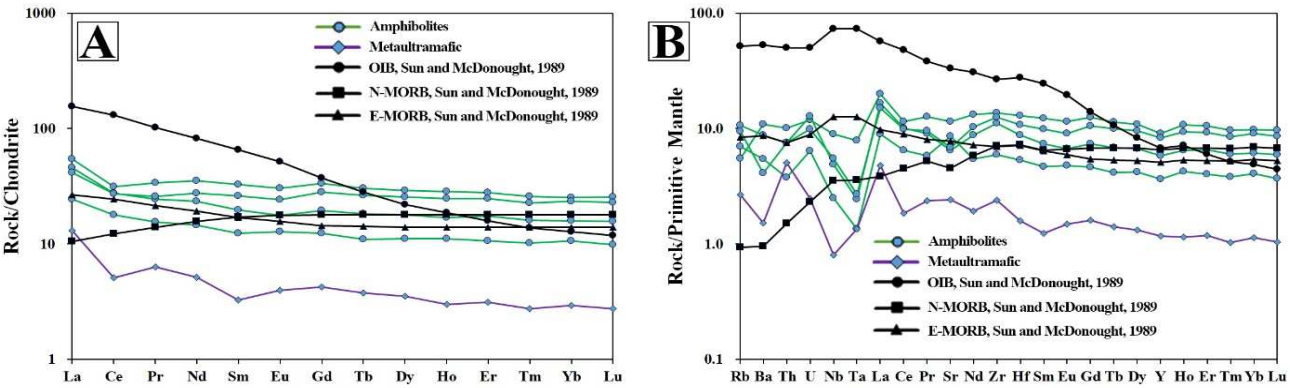

Figure 8 - Chondrite-normalized REE (A) and primitive mantle-normalized multi-element (B) patterns for the amphibolite and metaultramafic rock. Chondrite and normal mid-ocean ridge basalt (N-MORB), E-MORB and ocean island basalt (OIB) normalizing values data are after Sun & McDonough (1989). Primitive mantle normalizing values are after McDonough & Sun (1995).

The amphibolites have Zr concentrations varying of 62 to 143 ppm (113 ppm in average) and 3.66 to 4.66 Zr/Y ratio (3.99 in average), have 1.64 to 5.92 ppm of Nb (3.6 ppm in average) and 0.28 to 0.46 Nb/La ratios (0.35 in average), indicating some crustal contamination of the gabroic protholith according to to Xia (2014) and Xia et al. (2008). In the Y/Nb vs Zr/Nb diagram (Xia & Li, 2019), Th/Yb vs Nb/Yb diagram (Pearce, 2008) and Th_N vs Nb_N diagram (Saccani, 2015) respectively presented in Figures 9A, 9B, and 9C, show a transitional (T-MORB) to enriched (E-MORB) signature for the amphibolites, and this enrichment could be related to crustal contamination.

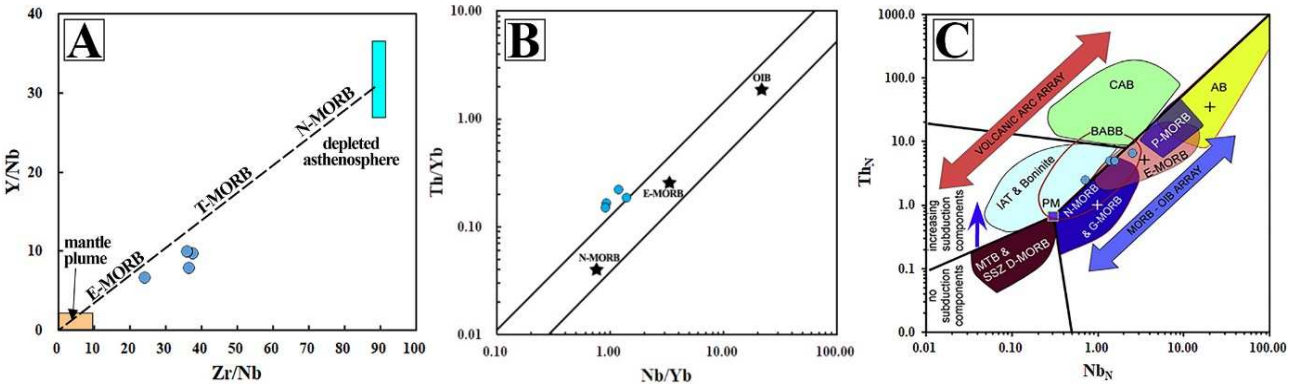

Figure 9 - (A) Y/Nb vs Zr/Nb (Xia & Li, 2019). (B) Th/Yb vs Nb/Yb (Pearce, 2008). (C) Th_N vs Nb_N (Nb and Th are normalized to the N-MORB composition from Sun & McDonough, 1989) (Saccani, 2015). T – Transitional. N – Normal. E – Enriched. G - garnet-influenced, AB - alkaline basalt, IAT - island arc tholeiite, CAB - calc-alkaline basalt, BABB – back-arc basin basalt. Only amphibolite samples were ploted.

In the Itapecerica region, metaultramafic rock and amphibolites occur near each other, in the same context to the rocks of the Itapecerica supracrustal succession, and nearby banded iron formations, whose protoliths are from oceanic basins and went through metamorphism of granulite facies conditions.

The anatexis of the amphibolites contributes to the generation of the Água Rasa Metagranite (Miranda et al., 2020) during the Rhyacian-Orosirian orogeny. Those conditions agree to the mineral paragenesis of the amphibolite, are suitable to crustal contamination from Itapecerica metasedimentary rocks, and the Nb and Ta anomalies can be related to fluid release from protolith during collision-related dehydration and incipient migmatization processes (Dey et al., 2018).

Geochemistry reveals high-Fe tholeiitic affinity for the amphibolite protolith with E-MORB signature. The association of amphibolites near metaperidotite in the region of Itapecerica, where rocks are from oceanic setting, suggests that the amphibolites and the metaultramafic could represent the transition of layered gabbros to ultramafic rocks in a typical ophiolite sequence, as shown in figure 10.

Chondrite-normalized REE and primitive mantle-normalized multi-element patterns for the amphibolite are very similar to that of metaultramafic rock (Figure 8) suggesting a genetic correlation between them. Therefore, it is reasonable to suggest that Itapecerica sequence keeps fragments of an ophiolite (Figure 10).

In the Tejuco Preto graphite mine (near Amp3 in Figure 2; Miranda et al., 2019) is possible to observe a morphological pattern that resembles pillow-like structures that could be from pillow lavas below the metasedimentary sequence (Figure 11). They are exposed upside down due to the fold character of the rocks in the mine, where layers are overturned. Unfortunately, due to the extremely weathered character, it was not possible to collect samples for petrography and geochemistry in order to investigate the ophiolitic proposition above.

CONCLUSION

The metaultramafic rock and amphibolites with E-MORB signature associated to the Itapecerica supracrustal succession rocks points to an oceanic setting.

Adjacent 2.1 Ga amphibolites from the CSZ (Goulart, 2006; Goulart & Carneiro, 2010) found in the same orogenic context also have E-MORB signature. A possible suture zone in the Itapecerica/Claudio region formed by the collision between Divinopolis and Campo Belo/Bonfim complexes during the Rhyacian-Orosirian orogeny involving the Itapecerica

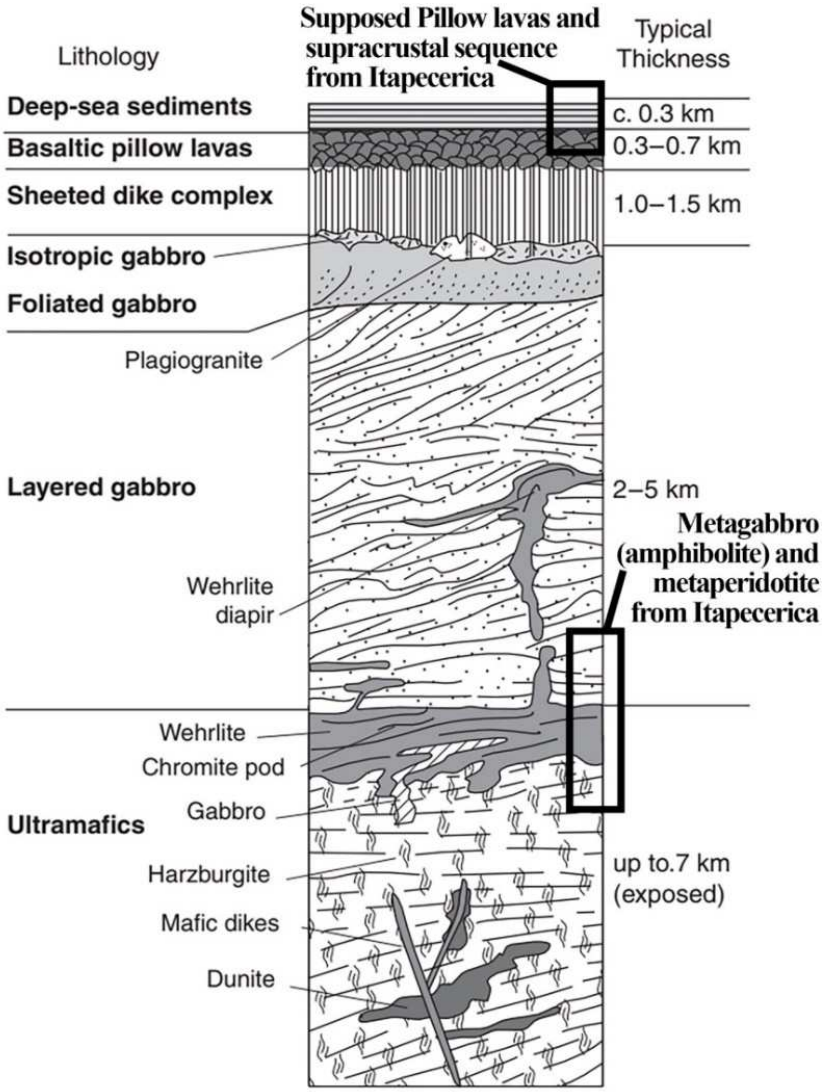

Figure 10 - Lithology and thickness of a typical ophiolite sequence (Winter, 2014).

Figure 11 - Morphological pattern that resembles pillow-shaped structures from supposed pillow lavas exposure in the Tejuco Preto graphite mine from Itapecerica-MG.

oceanic basin alongside CSZ (Coelho & Chaves, 2019) and forward to Minas Basin is a suggestive geological setting of the investigated region.

Even if those pillow-like morphological shapes are or not pillow, the association of the metaultramafic and amphibolites can be related to the mantle-oceanic crust transition.

ACKNOWLEDGMENTS

To the *Nacional de Grafite* Company, the geologist Lairton de Oliveira and geology supervisor Gilson dos Santos. This study was financed in part by the Coordenação de Aperfeiçoamento de Pessoal de Nível Superior - Brasil (CAPES) - Finance Code 001. The second author thanks to CNPq the research productivity grant and FAPEMIG for research support through the project APQ-00654-16.

REFERENCES

AGUILAR, C.; ALKMIM, F.F.; LANA, C.; FARINA, F. Palaeoproterozoic assembly of the São Francisco craton, SE Brazil: new insights from U–Pb titanite and monazite dating. **Precambrian Res**., v. 289, p. 95-115, 2017.

ÁVILA, C.A.; TEIXEIRA, W.; BONGIOLO, E.M.; DUSSIN, I.A.; VIEIRA, T.A.T. Rhyacian evolution of subvolcanic and metasedimentary rocks of the southern segment of the Mineiro belt, São Francisco Craton, Brazil. **Precambrian Res.**, v. 243, p. 221-251, 2014.

CAMPELLO, M.S.; VAZ, B.B.; OLIVEIRA, M.A.S.; ÁVILA, M.A.C. **Relatório e mapa geológicos 1:100.000 da Folha Formiga SF.23-V-B-III. Projeto Fortaleza de Minas,** CODEMIG/UFMG. A.C. Pedrosa Soares (coord.). 62 p., 2015.

CARNEIRO, M.A. & BARBOSA, M.S.C. Implicações geológicas e tectônicas da interpretação magnetométrica da região de Oliveira, Minas Gerais. **Revista Brasileira de Geofísica**, v. 26, n. 1, p. 87-98, 2008.

CARNEIRO, M.A.; NALINI JÚNIOR, H.A.; ENDO, I.; SUITA, M.T.F.; CASTRO, P.T.A.; BARBOSA, M.S.C.; CAMPOS, J.C.S.; GOULART, L.E.A.; SILVA, E.F.S.; PEREIRA, A.A.; TAVARES, T.D.; JIAMELARO, F.; CARNEIRO, J.M.; MARIANO, L.C.; MIGUEL, F.P.; SILVA JUNIOR, A.C.; BARBOSA, A.S.; PRADO, G.E.A.; SANTOS, C.; URBANO, E.E.M.C. **Folha Campo Belo- SF.23-V-B-VI, escala 1:100.000: nota explicativa integrada com Oliveira**. UFOP/CPRM, Minas Gerais, 114 p., 2007.

CARVALHO, B.B.; JANASI, V.A.; SAWYER, E.W. Evidence for Paleoproterozoic anatexis and crustal reworking of Archean crust in the São Francisco Craton, Brazil: a dating and isotopic study of the Kinawa migmatite. **Precambrian Res**., v. 291, p. 98-118, 2017.

CHAVES, A.O. Enxames de diques máficos de Minas Gerais – o estado da arte. **Geonomos**, v. 21, n. 1, p. 29-33, 2013.

CHAVES, A.O.; CAMPELLO, M.S.; SOARES, A.C.P. Idade U-Th-PbT de monazitas do sillimanita-cordierita-granada-biotita gnaisse de Itapecerica (MG) e a atuação da orogenia Riaciano-Orosiriana no interior do Cráton São Francisco Meridional. **Geociências**, v. 34, n. 3, p. 324-334, 2015.

COELHO, R.M. & CHAVES, A.O. Pressure-temperature-time path of Paleoproterozoic khondalites from Claudio shear zone (southern São Francisco craton, Brazil): Links with khondalite belt of the North China craton. **Journal of South American Earth Sciences**, v. 94, 2019, Doi: 102250.

DEY, A.; HUSSAIN, M.F.; BARMAN, M.N. Geochemical characteristics of mafic and ultramafic rocks from the Naga Hills Ophiolite, India: Implications for petrogenesis. **Geoscience Frontiers**, v. 9, p. 517-529, 2018.

DILEK, Y. & FURNES, H. Ophiolite genesis and global tectonics: geochemical and tectonic fingerprinting of ancient oceanic lithosphere. **Geological Society of America Bulletin**, v. 123, p. 387-411. 2011.

DRUMMOND, J.B.R.; PUFAHL, P.K.; PORTO, C.G.; CARVALHO, M. Neoproterozoic peritidal phosphorite from the Sete Lagoas Formation (Brazil) and the Precambrian phosphorous cycle. **Sedimentology**, v. 62, p. 1978-2008, 2015.

DUTRA, L.F.; MARTINS, M.; LANA, C. Sedimentary and U-Pb detrital zircons provenance of the Paleoproterozoic Piracicaba and Sabará groups, Quadrilátero Ferrífero, Southern São Francisco craton, Brazil. **Brazilian Journal of Geology**, v. 49, n. 2, p. 1-21, 2019.

FARINA, F.A.; ALBERT, C.; LANA, C. The Neoarchean transition between medium and high-K granitoids: clues from the Southern São Francisco Craton (Brazil). **Precambrian Res**., v. 266, p. 375-394, 2015.

FERNANDES, R.A. & CARNEIRO, M.A.O. Complexo Metamórfico Campo Belo (Craton São Francisco Meridional): unidades litodêmicas e evolução tectônica. **Revista Brasileira de Geociencias**, v.30, n. 4, p. 671-678, 2000.

GOULART, L.E.A. & CARNEIRO, M.A. Magmatismo máfico-ultramáfico Paleoproterozóico no cráton São Francisco meridional: a sequência acamadada Itaguara. In: 45º CONGRESSO BRASILEIRO DE GEOLOGIA, Belém, 2010. **Anais**...Belém: Sociedade Brasileira de Geologia.

GOULART, L.E.A. O complexo acamadado Itaguara-Rio Manso, MG. Ouro Preto, 2006. 186 p. Dissertação (Mestrado), Universidade Federal de Ouro Preto.

IRVINE, T. & BARAGAR, W. A guide to the chemical classification of the common volcanic rocks. **Canadian Journal of Earth Science**s, v. 8, n. 5, p. 523-548, 1971.

JENSEN, L.S. A new cation plot for classifying subalkaline volcanic rocks. **Ontario Division Mines Miscellaneous Paper** 66, 22 p., 1976.

MACHADO FILHO, L.; RIBEIRO, M.W.; GONZALEZ, S.R.; SCHENINI, C.A.; SANTOS NETO, A.S.; BARROS PALMEIRA, R.C.; PIRES, J.L.; TEIXEIRA, W.; CASTRO, H.E.F. **Geologia.** In: PROJETO RADAM BRASIL, Folhas SF 23/24, Rio de Janeiro/Vitória, v. 32, p. 36-45, 1983.

McDONOUGH, W.F. & SUN, S.S. The composition of the Earth. **Chemical Geology**, v. 67, n. 5, p. 1050-1056, 1995.

MIRANDA, D.A.; CHAVES, A.O.; CAMPELLO, M.S.; RAMOS, S.L.L.M. Origin and thermometry of graphites from Itapecerica supracrustal succession of the southern Sao Francisco Craton by C isotopes, X-ray diffraction and Raman spectroscopy. **International Geology Review**, v. 61, n. 15, p. 1864-1875, 2019.

MIRANDA, D.A.; CHAVES, A.O.; DUSSIN, I.A.; PORCHER, C.C. Paleoproterozoic khondalites in Brazil: a case study of metamorphism and anatexis in khondalites from Itapecerica supracrustal succession of the southern São Francisco Craton. **International Geology Review**, doi:10.1080/00206814.2020. 1716273, 2020.

MOREIRA, H.; SEIXAS, L.; STOREY, C.; FOWLER, M.; LASALLE, S.; STEVENSON, R.; LANA, C. Evolution of Siderian juvenile crust to Rhyacian high Ba-Sr magmatism in the Mineiro belt, southern São Francisco Craton. **Geoscience Frontiers**, v. 9, p. 977-995, 2018.

NERI, M.E.N.V.; ROSIÈRE, C.A.; LANA, C.C. Supergrupo Minas na Serra de Bom Sucesso, extremo sudoeste do Quadrilátero Ferrífero – MG: petrografia, geoquímica e isótopos de U-Pb. **Revista Geologia USP Série Científica**, v. 13, n. 2, p. 117-202, 2013.

NOCE, C.M.; MACHADO, N.; TEIXEIRA, W. U-Pb

Geochronology of gneisses and granitoids in the Quadrilatero Ferrıfero (Southern São Francisco Craton): age constraints for Archean and Paleoproterozoic magmatism and metamorphism. **Revista Brasileira de Geociencias**, v. 28, p. 95-102, 1998.

NOCE, C.M.; PEDROSA-SOARES, A.C.; SILVA, L.C.; ARMSTRONG, R.; PIUZANA, D. Evolution of polycyclic basement in the Araçuaí Orogen based on U-Pb SHRIMP data: implications for the Brazil-Africa links in the Paleoproterozoic time. **Precambrian Res**., v. 159, p. 60-78, 2007.

OLIVEIRA, A.H. Evolução tectônica de um fragmento do Cráton São Francisco Meridional com base em aspectos estruturais, geoquímicos (rocha total) e geocronológicos (Rb-Sr, Sm-Nd, Ar-Ar, U-Pb). Ouro Preto, Brazil, 2004. 92 p. Tese (Doutorado), Universidade Federal de Ouro Preto, Brazil.

PEARCE, J.A. Geochemical fingerprinting of oceanic basalts with applications to ophiolite classification and the search for Archean oceanic crust. **Lithos**, v.100, p.14–48, 2008.

RUY, A.C.; SILVA, A.M.; TOLEDO, C.L.B.; SOUZA FILHO, C.R. Uso de dados aerogeofísicos de alta densidade para mapeamento geológico em terrenos altamente intemperizados: o estudo de caso da região de Cláudio, porção sul do Cráton São Francisco. **Revista Brasileira de Geofísica**, v. 24, n. 4, p. 535-546, 2006.

SACCANI, E. A new method of discriminating different types of post-Archean ophiolitic basalts and their tectonic significance using Th-Nb and Ce-Dy-Yb systematics. **Geoscience Frontiers**, v. 6, p. 481-501, 2015.

SHERVAIS, J.W. Ti-V plots and the petrogenesis of modern ophiolitic lavas. **Earth and Planetary Science Letters**, v. 59, n. 1, p. 101–118, 1982.

STRECKEISEN, A.L. Classification and Nomenclature of Plutonic Rocks. Recommendations of the IUGS Subcommission on the Systematics of Igneous Rocks. **Geologische Rundschau. Internationale Zeitschrift für Geologie**. Stuttgart, v. 63, p. 773-786, 1974.

SUN, S.S. & McDONOUGH, W.F. Chemical and isotopic systematics of oceanic basalts, implications for mantle composition and processes. In: Saunders, A. D., Norry, M. J., (Ed.). Magmatism in the ocean basins. **Geological Society of London**, London, v. 42, p. 313-345, 1989.

TEIXEIRA, W.; CARNEIRO, M.A.; NOCE, C.M.; MACHADO, N.; SATO, K.; TAYLOR, P.N. Pb, Sr and Nd isotope constraints on the Archean evolution of the gneissic-granitoid in the southern São Francisco Craton, Brazil. **Precambr. Res.**, v. 78, p. 151-164, 1996.

TEIXEIRA, W.; ÁVILA, C.A.; DUSSIN, I.A.; NETO, A.C.; BONGIOLO, E.M.; SANTOS, J.O.; BARBOSA, N.S. A juvenile accretion episode (2.35–2.32 Ga) in the Mineiro belt and its role to the Minas accretionary orogeny: zircon U-Pb-Hf and geochemical evidences. **Precambr. Res**., v. 256, p. 148-169, 2015.

TEIXEIRA, W.; OLIVEIRA, E.P.; PENG, P.; DANTAS, E.L.; HOLLANDA, M.H.B.M. U-Pb geochronology of the 2.0 Ga Itapecerica graphite-rich supracrustal succession in the São Francisco Craton: Tectonic matches with the North China Craton and paleogeographic inferences. **Precambrian Research**, v. 293, p. 91-111, 2017a.

TEIXEIRA, W.; OLIVEIRA, E.P.; MARQUES, L.S. The nature and evolution of the Archean Crust of the São Francisco Craton. In: HEILBRON, M.; ALKMIM, F.; CORDANI, U.G. (Eds). SÃO FRANCISCO CRATON, EASTERN BRASIL: TECTONIC GENEALOGY OF A MINIATURE CONTINENT, **Regional Geology Review Series.** Springer-Verlag, p. 29-56, 2017b.

WHITNEY, D.L. & EVANS, B.W. Abbreviations for names of rock-forming minerals. **American Mineralogist**, v. 95, n. 1, p.185-187, 2010.

WINTER, J.D. **Principles of Igneous and Metamorphic Petrology**. Pearson Education, 2 ed., 744 p., 2014.

XIA, L. & LI, X. Basalt geochemistry as a diagnostic indicator of tectonic setting. **Gondwana Research**, v. 65, p. 43-67, 2019.

XIA, L.Q. The geochemical criteria to distinguish continental basalts from arc related ones. **Earth-Science Reviews**, v. 139, p. 195-212, 2014.

XIA, L.Q.; XIA, Z.C.; XU, X.Y.; LI, X.M.; MA, Z.P. Relative contributions of crust and mantle to the generation of the Tianshan Carboniferous rifrelated basic lavas, northwestern China. **Journal of Asian Earth Sciences**, v. 31, n. 4-6, p.357-378, 2008.

ZACCHI, E.N.P.; SILVA, A.M.; TOLEDO, C.L.B.; SOUZA FILHO, C.R. As três anomalias elípticas da porção sul do Cráton São Francisco: novos alvos para a mineralização de grafita? **Revista Brasileira de Geofísica**, v. 25, n. 4, p. 421-431, 2007.

ZHANG, Q.; SUN, W.; ZHAO, Y.; YUAN, F.; JIAO, S.; CHEN, W. New discrimination diagrams for basalts based on big data research. Big Earth Data, v. 3, n.1, p. 45-55, 2019.

ZHOU, J. & LI, X. GeoPlot: an excel VBA program for geochemical data plotting. **Computers and Geosciences**, v. 32, p. 554-560, 2006.

Submetido em 28 de agosto de 2020
Aceito para publicação em 5 de janeiro de 2021